



**Nanochitosan crosslinked with polyacrylamide as the chiral stationary phase for open-tubular capillary electrochromatography**

Journal:	<i>Electrophoresis</i>
Manuscript ID:	elps.201000410.R2
Wiley - Manuscript type:	Research Paper
Date Submitted by the Author:	n/a
Complete List of Authors:	Chen, Jian-Lian; China Medical University, School of Pharmacy Hsieh, Kai-Hsin; China Medical University, School of Pharmacy
Keywords:	Capillary electrochromatography, Chitosan, Chiral stationary phase, Nanoparticles, Open-tubular, Polyacrylamide

SCHOLARONE™  
Manuscripts

1  
2  
3 1 **Nanochitosan crosslinked with polyacrylamide as the chiral stationary**  
4  
5 2 **phase for open-tubular capillary electrochromatography**  
6  
7

8  
9 3

10  
11 4 Jian-Lian Chen\*, Kai-Hsin Hsieh

12  
13 5 School of Pharmacy, China Medical University, Taichung, Taiwan  
14  
15  
16 6  
17  
18 7

19  
20 8 **Correspondence:** Dr. Jian-Lian Chen, School of Pharmacy, China Medical University, No.91

21  
22 9 Hsueh-Shih Road, Taichung 40402, Taiwan  
23  
24

25 10 **E-mail:** cjl@mail.cmu.edu.tw

26  
27 11 **Fax:** +886-4-22031075  
28

29  
30 12 **Abbreviations:** ACN, acetonitrile; AIBN, 2,2'-azobis(2-methylpropionitrile); BHT,

31  
32 13 butylhydroxytoluene; Bis, N,N'-methylenebisacrylamide; CEC, capillary

33  
34 14 electrochromatography; CS, chitosan; CSP, chiral stationary phase; DMSO,

35  
36 15 dimethylsulfoxide; DPPH, 2,2-diphenyl-1-picryl-hydrazyl; EtOH, ethanol; GMA, glycidyl

37  
38 16 methacrylate;  $k''$ , retention factor;  $k_e''$ , velocity factor; MAA, methacrylamide;  $\gamma$ -MAPS,

39  
40 17 3-(trimethoxysilyl) propylmethacrylate; OT, open tubular; PVA, polyvinyl alcohol; Tris,

41  
42 18 tris(hydroxymethyl)aminomethane  
43  
44  
45  
46  
47  
48  
49  
50  
51  
52  
53  
54  
55  
56  
57  
58  
59  
60

1  
2  
3  
4 **1 Abstract**

5  
6 2 Nanoparticles exhibiting favorable surface-to-volume ratios create efficient stationary phases  
7  
8 3 for electrochromatography. New nanomaterials derived from chitosan (CS) were immobilized  
9  
10 4 onto modified capillaries for use as the chiral stationary phase (CSP) in open-tubular  
11  
12 5 electrochromatography. This immobilization was achieved through the copolymerization of  
13  
14 6 glycidyl methacrylate-modified nano-CS with methacrylamide (MAA) and bis-acrylamide  
15  
16 7 crosslinkers (forming the MAA-CS capillary) rather than the attachment of nano-CS to the  
17  
18 8 copolymer of GMA, MAA, and bis-acrylamide (forming the MAA+CS capillary). The  
19  
20 9 completed MAA-CS capillary and its precursors were examined by SEM and ATR-IR  
21  
22 10 measurements. Before separating chiral samples, the MAA-CS capillary was characterized by  
23  
24 11 electroosmotic flow measurements at varying pH values, concentrations, and volume  
25  
26 12 percentages of organic modifiers in the running buffers. Tryptophan enantiomers were well  
27  
28 13 separated by the MAA-CS capillary, whereas no enantioselectivity was observed in the  
29  
30 14 MAA+CS capillary. With the addition of 80% MeOH into the phosphate buffer, the chiral  
31  
32 15 separation of ( $\pm$ )-catechin was accomplished in a normal-phase mode. However, the new CSP  
33  
34 16 has its limitations, as only two groups of  $\alpha$ -tocopherol stereoisomers were separated.  
35  
36  
37  
38  
39  
40  
41  
42

43 **18 Keywords:** Capillary electrochromatography / Chiral stationary phase / Chitosan /  
44  
45 19 Nanoparticles / Open-tubular / Polyacrylamide /  
46  
47  
48  
49  
50  
51  
52  
53  
54  
55  
56  
57  
58  
59  
60

## 1 Introduction

Growth in chiral separation techniques is based on the continued development of new chiral stationary phases (CSPs) and better mechanistic understandings of them. Among these techniques, capillary electrochromatography (CEC) providing various column technologies is well-suited to the discovery of new phases with proper formats, and its many successful implementations for enantiomer separations are often reviewed [1–4]. Traditionally, CSPs or chiral selectors used in HPLC columns have been used in CEC, which has resulted in the production of three major categories of column technologies: packed, open-tubular (OT), and monolithic columns.

Due to the lack of phase ratios, the OT column format attracts less attention compared to the other two column technologies. However, it is a comparatively straightforward approach that does not require the arduous fabrication of any frits that is required in particulate-packed column creation or the blending of monomer reagents with suitable porogens in precise proportions that is required for monolith. Strategies to increase the loadability of the designed chiral selectors have been developed and include the techniques of polyelectrolyte multilayer coating [5–7], layer-by-layer assembly [8,9], high-affinity incorporation into bilayers [10,11], and immobilization on silica gel or organic polymer gel as achiral supported layers (brush-type CSPs) [12–15]. The OT-CEC capillaries modified with chemically bonded chiral selectors have longer lifetimes and better reproducibilities than capillaries with physical coatings that were created by any of the first three strategies. In addition to brush-type CSPs, chiral selectors are chemically bonded to the polymer-type CSPs. Examples of OT-CEC capillaries with polymer-type CSPs are a molecular imprinted polymer [16–18] and a bonding of avidin protein [19,20].

Nanoparticles exhibiting favorable surface-to-volume ratios create efficient stationary phases for electrochromatography [21]. Some nanomaterials (including silica [22], titanium oxide [23,24], gold [25], and carbon nanotubes (CNT) [26,27]) have previously been

1  
2  
3  
4 1 chemically immobilized in OT-CEC capillaries. In a similar manner, chiral nanoparticles are  
5  
6 2 potential CSPs for use in enantioseparations. Chitosan (CS) particulates and their derivatives  
7  
8 3 have been employed in a wide range of biomedical applications including drug-delivery and  
9  
10 4 gene-delivery systems [28,29], and their natural properties meet the requirements of  
11  
12 5 polymer-type CSP. Chitosan, poly- $\beta$ -(1,4)-2-acetamido-2-deoxy-D-glucopyranose is a  
13  
14 6 functional linear polysaccharide and the *N*-deacetylated derivative of chitin, the second most  
15  
16 7 abundant biopolymer in nature. Because of its specific basic properties, CS and its derivatives  
17  
18 8 have mainly been used as coating reagents that were adsorbed on bare capillaries to separate  
19  
20 9 bioactive molecules by OT-CEC [30,31]. For enantiomeric separations by CEC using  
21  
22 10 CS-immobilized CSPs, a monolithic phase composed of sol-gel/organic hybrid materials  
23  
24 11 containing CS and bovine serum albumin (BSA) has been the only successful example studied  
25  
26 12 to date [32]. Here, BSA and CS both are possessed of chiral selectivity. As regards HPLC,  
27  
28 13 CS-immobilized CSPs have been successfully applied in some studies [33-35].  
29  
30  
31  
32  
33

34 14 In this study, CS nanoparticles prepared by a precipitation method were copolymerized  
35  
36 15 with methacrylamide (MAA) monomers and *N,N'*-methylenebisacrylamide crosslinkers (Bis)  
37  
38 16 to create an OT-CEC capillary with CSP functionality. The complete MAA-CS capillary and  
39  
40 17 its precursor materials were characterized by SEM and ATR-IR. Further, the effects on its  
41  
42 18 electroosmotic mobilities ( $\mu_{eo}$ ) caused by changes in pH values, buffer concentrations, and the  
43  
44 19 volumetric addition of organic modifiers to the running buffers were investigated. Chiral  
45  
46 20 samples including tryptophan, catechin, and  $\alpha$ -tocopherol were prepared to test the CSP  
47  
48 21 functionality of the new capillaries.  
49  
50  
51  
52  
53

## 54 23 **2 Materials and methods**

### 55 24 **2.1 Reagents and chemicals**

56  
57 25 Most chemicals used were of analytical or chromatographic grades. Chitosan (CS; from  
58  
59 26 shrimp shells, practical grade,  $\geq 75\%$  deacetylated), 2,2-diphenyl-1-picryl-hydrazyl (DPPH),  
60

1  
2  
3  
4 1 methacrylamide (MAA), N,N'-methylenebisacrylamide (Bis), glycidyl methacrylate (GMA),  
5  
6 2 2,2'-azobis(2-methylpropionitrile) (AIBN), sodium tetraborate, phosphoric acid, sodium  
7  
8 3 dihydrogenphosphate, hydrochloric acid, acetonitrile (ACN), and dimethylsulfoxide (DMSO)  
9  
10 4 were purchased from Sigma–Aldrich (Milwaukee, WI, USA). Boric acid, acetic acid,  
11  
12 5 ammonium carbonate, methylene chloride, methanol and ethanol (EtOH) were obtained from  
13  
14 6 Panreac Quimica S.A. (Barcelona, Spain). Sodium hydroxide, butylhydroxytoluene (BHT),  
15  
16 7 polyvinyl alcohol (PVA), disodium hydrogenphosphate, tri-sodium phosphate, citric acid,  
17  
18 8 sodium dihydrogen citrate, disodium hydrogen citrate, and trisodium citrate were supplied by  
19  
20 9 Merck (Garmstadt, Germany). Acetone, sodium sulfate, sodium acetate were obtained from  
21  
22 10 Mallinckrodt Baker (Phillipsburg, NJ, USA). Tris(hydroxymethyl)aminomethane (Tris) was  
23  
24 11 received from TEDIA (Carson City, CA, USA). The chemical 3-(trimethoxysilyl)  
25  
26 12 propylmethacrylate ( $\gamma$ -MAPS) was obtained from Acros Organics (Geel, Belgium). Finally,  
27  
28 13 *m*-Methylbenzoic acid was purchased from TCI (Tokyo, Japan).

29  
30  
31  
32  
33  
34 14 The chiral analytes consisted of tryptophans (L, D, and DL forms), the catechins of  
35  
36 15 (+)-(2R,3S)- and  
37  
38 16 (–)-(2S,3R)-2-(3,4-dihydroxyphenyl)-3,4-dihydro-1(2H)-benzopyran-3,5,7-triol, and the  
39  
40 17  $\alpha$ -tocopherols of (+)-2*R*,4'*R*,8'*R*- $\alpha$ -tocopherol and its racemate ( $\pm$ ). Their respective chemical  
41  
42 18 structures are illustrated in Fig. 1. All chiral analytes were purchased from Sigma–Aldrich  
43  
44 19 (Milwaukee, WI, USA). Sample concentrations were 1.0 mg/mL tryptophan in H<sub>2</sub>O, 25  
45  
46 20  $\mu$ g/mL catechins in MeOH, and 10 mg/mL vitamin E in a preservation solution (98 ml MeOH,  
47  
48 21 2 ml H<sub>2</sub>O and 5 mg BHT). Purified water (18 M $\Omega$  cm) from a Milli-Q water purification  
49  
50 22 system (Millipore, Bedford, MA, USA) was used to prepare samples and buffer solutions.

## 51 23 **2.2 Instrumentation**

52  
53  
54  
55  
56  
57 24 The laboratory-built electrophoresis apparatus consisted of a  $\pm$ 30 kV high-voltage power  
58  
59 25 supply (Model: TriSep TM-2100, Unimicro Technologies, CA, USA) and a UV-Vis detector  
60  
26 (Model: LCD 2083.2 CE, ECOM, Prague, Czech). Electrochromatograms were recorded

1 using a Peak-ABC Chromatography Data Handling System (Kingtech Scientific, Taiwan). A  
2 Joel JSM-6700F Scanning Microscopy at National Chung Hsing University acquired the SEM  
3 images at an accelerating voltage of 3.0 kV. The ATR-IR spectra were obtained by a  
4 Shimadzu Prestige-21 IR spectrometer (Kyoto, Japan) that was equipped with a single  
5 reflection horizontal ATR accessory (Model: MIRacle, PIKE Technologies, WI, USA).

### 6 **2.3 Preparation of capillary columns**

7 The scheme of major reactions concerning with the synthesis of the CS-immobilized capillary  
8 is shown in Fig. 2.

#### 9 **2.3.1 Preparation and derivatization of CS nanoparticles**

10 According the precipitation method [36], CS (0.25%, w/v) was dissolved in an aqueous  
11 solution of acetic acid (2%, v/v) containing PVA (10%, w/v). Sodium sulfate solutions (20%,  
12 w/v) were added dropwise (5 mL/min) to CS solutions while stirring at 400 rpm under  
13 ultrasonication. After adding sodium sulfate solutions, stirring and sonication were continued  
14 for another 1 h. CS nanoparticles (nano-CS) were collected by centrifugation at 3000 rpm,  
15 rinsed for several times with distilled water until the pH value decreased to 7, and dried at  
16 80°C for 1 day.

17 The purified, dry nano-CS (5 mg), *m*-methylbenzoic acid (50 mg), and potassium acetate  
18 (50 mg) were dispersed in methylene chloride (5 mL) at room temperature for 6 h under  
19 ultrasonication. The resulting acid-treated nano-CS could be easily obtained by evaporating  
20 the methylene chloride and wash with water for the measurements of SEM and ATR-IR. For  
21 attaching vinyl groups on the nano-CS, the GMA (5 mL) reagent was directly added into the  
22 above methylene chloride mixture and reacted at 60°C for 2 h under ultrasonication. After  
23 the derivatization, the GMA-nano-CS derivative with allyl groups was obtained and offered  
24 its reactivity during the polymerization required for MAA-CS column preparation.

#### 25 **2.3.2 Preparation of MAA-CS and MAA+CS capillaries**

26 The preparation of a silanized phase proceeded according to previously described protocols

1  
2  
3  
4 1 [27]. A new, bare capillary column (Polymicro Technologies, Phoenix, AZ, USA) with  
5  
6 2 375- $\mu\text{m}$  O.D. x 75- $\mu\text{m}$  I.D. was treated with 1.0 M NaOH and successively washed with  
7  
8 3 pure water, 0.1 M HCl, pure water, and then acetone. The clean, bare capillary was then  
9  
10 4 filled with a solution composed of DPPH (0.02 g),  $\gamma$ -MAPS (1.0 mL), and MeOH (1.0 mL).  
11  
12 5 This capillary was kept at room temperature for 24 h to undergo the silanization, which was  
13  
14 6 completed after a series of rinses with MeOH, H<sub>2</sub>O, and acetone.  
15  
16

17  
18 7 For preparation of the MAA-CS capillary, a polymerization solution was mixed with  
19  
20 8 MAA (0.03 mol), Bis (0.01 mol), AIBN (30 mg), and GMA-nano-CS derivatives (3 mL of  
21  
22 9 methylene chloride solution). After the silanized capillary was filled with the polymerization  
23  
24 10 solution, most of the mixed solution was purged out of capillary by blowing nitrogen  
25  
26 11 through the tube at 40 psi for 5 min, but a thin layer of solution was left on the capillary wall  
27  
28 12 that was ready to react with the silanized capillary. The capillary was left at room  
29  
30 13 temperature for 30 min to complete the polymerization reaction. Finally, the completed  
31  
32 14 MAA-CS capillary was washed successively with H<sub>2</sub>O, ethanol, and acetone for 30 min. It  
33  
34 15 was then ready for CEC testing.  
35  
36  
37

38  
39 16 For the preparation of the MAA+CS capillary, a silanized capillary was filled with a  
40  
41 17 polymerization solution containing MAA (0.03 mol), Bis (0.01 mol), AIBN (30 mg), and  
42  
43 18 GMA (3 mL). After purging at 40 psi for 5 min, the capillary was stored at room temperature  
44  
45 19 for 30 min. A portion of the methylene chloride solution (5 mL) containing 5 mg of CS  
46  
47 20 nanoparticles, *m*-methyl benzoic acid (50 mg), and potassium acetate (50 mg) was put inside  
48  
49 21 the capillary. The capillary was plugged with a septum and placed in an oven at 60°C for 2 h.  
50  
51 22 Finally, the completed MAA+CS capillary was cleaned in the same way as the MAA-CS  
52  
53 23 capillary.  
54  
55

#### 56 57 24 **2.4 CEC conditions**

58  
59 25 Most experiments were conducted using the common CZE buffers of Tris, acetate, citrate,  
60  
26 phosphate, ammonium carbonate, and borate buffers within a pH range of 5.0 to 10.5 and an



1 ionic concentration range of 10 to 300 mM. ACN and MeOH were used as organic modifiers  
2 added in the buffers. All prepared buffer solutions for CEC analysis were filtered through a  
3 0.45- $\mu$ m cellulose ester membrane (Adventec MFS, Pleasanton, CA, USA). DMSO was used  
4 as the neutral marker. At the end of the analysis, the studied capillary was washed with  
5 methanol, pure water, and running buffer, sequentially, between each run. Prior to a sample  
6 injection, a working voltage was applied for 5 min to condition the charge distribution in the  
7 column. The prepared test samples were introduced by siphoning using a height difference.  
8 The samples were detected by UV light absorption measurements at 214 nm for DMSO, 214  
9 nm for tryptophans, 280 nm for catechins, and 200 nm for vitamin E.

### 11 **3 Results and discussion**

#### 12 **3.1 Characterization of MAA-CNT phase**

##### 13 **3.1.1 SEM images and ATR-IR spectra**

14 The nano-CS was primarily prepared by a precipitation method and was reported with the size  
15 distribution ranging from 40 to 100 nm measured by TEM micrographs [36]. Afterward the  
16 amino end groups of nano-CS reacted with *m*-methyl benzoic acid in methylene chloride  
17 under ultrasonication. This amidization increased the hydrophobicity of CS chains, which  
18 tended to be straightened due to the intermolecular interactions with concurrent  
19 self-association of *m*-methyl benzoic acid units of neighboring chains. The sizes of the CS  
20 self-aggregates were mainly controlled by the molecular weight of the CS backbone chains.  
21 According to the study on deoxycholic acid-modified CS, its self-aggregates may form a  
22 cylindrical bamboolike structure when the chitosan backbone is higher than 40 kDa and had  
23 the mean diameter in the range of 130-300 nm measured by dynamic light scattering method  
24 [37]. In Fig. 3(A), the SEM image of *m*-methyl benzoic acid-treated nano-CS shows the  
25 bamboolike structure with aggregation of some basic rod-like units, which diameter was  
26 nearly 150 nm. The ATR-IR spectrum of the acid-treated nano-CS is shown in Supporting

1  
2  
3  
4 1 information. The ATR-IR peaks correspond to an amide bond formation between the amine  
5  
6 2 groups of CS and the acid groups of the *m*-methyl benzoic acid.  
7  
8 3 The acid-treated nano-CS was further modified with GMA to anchor vinyl groups on the CS  
9  
10 4 chain. This modification required an epoxide ring-opening reaction and proceeded from the  
11  
12 5 nucleophilic attack of the CS hydroxyl groups. The ATR-IR of the resulting products,  
13  
14 6 GMA-nano-CS, is shown in Supporting information. The prepared GMA-nano-CS was added  
15  
16 7 to the polymerization solution that was ready for free-radical polymerization. This  
17  
18 8 polymerization occurred in a beaker and in the silanized capillary. The SEM images of the  
19  
20 9 polyacrylamide/nano-CS composite present in the beaker and in the capillary are shown in  
21  
22 10 Fig. 3(B) and 3(C), respectively. In both images, acrylamide polymers tied bundles of  
23  
24 11 bamboolike nano-CS together. The C=C bonds in GMA-nano-CS and  $\gamma$ -MAPS, a silanizing  
25  
26 12 agent bonding on a capillary, were successfully engaged in the polymerization of MAA in a  
27  
28 13 close silanized capillary as in an open beaker without the engagement of  $\gamma$ -MAPS. Inner  
29  
30 14 surface microphotographs of a length of ground MAA-CS capillary were taken and are shown  
31  
32 15 in Fig. 3(D). Some bundles of nano-CS were still attached to the capillary, but many were lost  
33  
34 16 during grinding. A scatter of rod-like CS particles was observed in the right bottom of Fig.  
35  
36 17 3(D). For the MAA-CS capillary shown in Supporting information, no IR absorption was  
37  
38 18 found at  $1640\text{ cm}^{-1}$ . This result means that the vinyl groups of all involved monomers were  
39  
40 19 completely used. Further, some absorption peaks were found between  $1050$  and  $1110\text{ cm}^{-1}$ ,  
41  
42 20 which correspond to the Si–O stretching mode, and around  $1700\text{ cm}^{-1}$ , which correspond to  
43  
44 21 the C=O stretching in the polyacrylamide phase.  
45  
46  
47  
48  
49  
50  
51

### 52 22 **3.1.2 The EOF profiles with varying buffer pHs, ionic strengths, and ratios of organic** 53 54 23 **modifier**

55  
56  
57 24 Before applying the MAA-CS capillary for electrochromatography and the chiral analyses, the  
58  
59 25 characterization of the EOF driven by the capillary under different buffer conditions was  
60  
26 performed. Some of the chemical properties of the MAA-CNT phase were revealed by these

1  
2  
3  
4 1 measurements. The two curves shown in Fig. 4(A) illustrate the dependence of  $\mu_{eo}$  on the pH  
5  
6 2 levels of the phosphate buffer for both the bare fused-silica capillary and the MAA-CS  
7  
8 3 capillary. Although the curve patterns of the MAA-CS were not the same as those of the bare  
9  
10 4 capillary, the effect of the residual silanol groups on the surface charges of the MAA-CS  
11  
12 5 capillary should be taken into consideration, which is especially true when the completeness  
13  
14 6 ratio for the silanization using  $\gamma$ -MAPS reagent was only around 20% [38]. The dissociation  
15  
16 7 of the residue silanols was more hindered by the coating layers of MAA-CS than the free  
17  
18 8 silanols on a bare capillary as the EOF of a bare capillary exceeded that of the MAA-CS  
19  
20 9 capillary at the high pH levels (pH > 9). The hydrogen of the silanols might be associated  
21  
22 10 with some atoms, such as oxygen and nitrogen, on the MAA-CS layers through hydrogen  
23  
24 11 bonding, and thus resulted in an EOF profile different from that of a bare capillary. Due to  
25  
26 12 conversion of the amine groups on the nano-CS to amide derivatives by their reaction with  
27  
28 13 *m*-methyl benzoic acid, the positive charge that formed on the MAA-CS phase surface could  
29  
30 14 be largely reduced. Similar phase structures and cathodic EOF patterns were found in CEC  
31  
32 15 columns with immobilized polysaccharides [39,40].

33  
34  
35  
36  
37  
38 16 The dependence of the EOF mobility on the logarithmic electrolyte concentration is  
39  
40 17 known to be linear in open tubes with thin double layers [41-43]. The trend of the curve of  $\mu_{eo}$   
41  
42 18 values along with the log *C* axis for the bare fused-silica and MAA-CS capillaries is shown in  
43  
44 19 Fig. 4(B). For the MAA-CS column, one point at the 10-mM concentration did not fit the line.  
45  
46 20 This phenomenon can be explained by the presence of a surface conductance, which could  
47  
48 21 induce the buildup of excess local charge in the double layer. The double layer might then slip  
49  
50 22 under the influence of the electric field applied to the tortuous surfaces, which were caused by  
51  
52 23 the modification process [44,45]. These overlapping double layers contributed to the  
53  
54 24 deviations from linearity and from the estimated slope value of  $-2 \times 10^{-4} \text{ cm}^2 \text{ V}^{-1} \text{ S}^{-1} \text{ mM}^{-1}$   
55  
56 25 [43]. In the range from 30 mM to 100 mM, the curve for the MAA-CS capillary was linear  
57  
58 26 ( $R^2 = 0.9373$ , slope =  $-14 \times 10^{-4} \text{ cm}^2 \text{ V}^{-1} \text{ S}^{-1} \text{ mM}^{-1}$ ). In this same range, the bare fused-silica

1  
2  
3  
4 1 capillary curve was also linear (0.9382, -3.3) [38]. The slope value of  $-14 \times 10^{-4}$  is far from  
5  
6 2 the estimated value of  $-2 \times 10^{-4}$  and is much larger than the slope value of  $-8.2 \times 10^{-4}$  that is  
7  
8 3 predicted for a PLOT capillary with a polyacrylate phase [38]. This difference is considered to  
9  
10 4 be a manifestation of the “openness” of the column, as packed columns typically have higher  
11  
12 5 negative slopes than OT columns [46].

13  
14  
15 6 The effect of adding the organic solvents of ACN and MeOH in the buffer solution on the  
16  
17 7  $\mu_{eo}$  values is highlighted in Fig. 4(C), which shows the presence of concave curves that have  
18  
19 8 minimums around 40-60% volume content of organic modifier. A similar trend is observed in  
20  
21 9 many OT-CEC formats including direct polymer coating, stepwise fabrication, and in-situ  
22  
23 10 polymerization [47–49,38]. This is primarily the result of a change in the ratio of the  
24  
25 11 dielectric constant to the viscosity of the running buffer (see the  $Y_2$  axis in Fig. 4(C)). This  
26  
27 12 situation suggests that the DMSO solute was a good EOF probe and that its chromatographic  
28  
29 13 interactions with the modified phases could be ignored.

30  
31  
32  
33  
34 14 The reproducibility of the capillary fabrication was evaluated from the  $\mu_{eo}$  values  
35  
36 15 measured at pH 7.6 for five runs of the MAA-CS capillary. The RSD values were 3.3, 3.7, and  
37  
38 16 4.2% for three newly replicated capillaries. At the 95% confidence level, no significant  
39  
40 17 differences between the columns were observed by *t*-test. The MAA-CS capillaries could be  
41  
42 18 used for more than 400 times within 6.0% RSD in half a year in the studies on the chiral  
43  
44 19 separations of different samples under various running buffers across wide pH ranges (pH  
45  
46 20 2–10) and volume ratios of organic modifier (5–100%). This indicated the fabrication of the  
47  
48 21 modified capillaries was pretty robust.

### 52 22 **3.2 Separation of tryptophan enantiomers**

53  
54  
55 23 Tryptophan enantiomers were used as chiral probes to assess the CEC enantioselectivities of  
56  
57 24 the MAA-CS and MAA+CS capillaries. After trying several buffers (described in section 2.4),  
58  
59 25 the best peak shape and resolution of racemic tryptophan were achieved with a Tris buffer  
60  
26 system using the MAA-CS capillary. The electropherograms shown in Fig. 5(A), (B), and (C)

1  
2  
3  
4 1 resulted from use of the Tris running buffer at a fixed molarity (100 mM) with different pH  
5  
6 2 values (pH = 8.5, 9.5, and 10.5). Figure 4(B) demonstrates the buffer at pH 9.5, which had a  
7  
8 3 much more satisfactory resolution than either pH 8.5 or 10.5. Changing the buffer  
9  
10 4 concentration from 50 mM to 200 mM verified the suitability of using a 100-mM  
11  
12 5 concentration. An organic modifier, MeOH, was added to the Tris buffer (pH 9.5, 100 mM)  
13  
14 6 but did not increase the selectivity (Fig. 5(D)).  
15  
16

17  
18 7 In another report by Kato et al. [32], a CSP composite of sol-gel, bovine serum albumin,  
19  
20 8 and chitosan for monolithic CEC of enantiomeric tryptophans reached the  $\alpha'$  values,  $t_D/t_L =$   
21  
22 9 1.10–1.15, higher than 1.02 obtained in the conditions of Fig. 5(B), but Kato et al. considered  
23  
24 10 the enantioselectivity by chitosan was negligible. However, our MAA-CS capillary had  
25  
26 11 higher theoretical plate numbers of tryptophans, 650,000 and 930,000 (N/m), than the  
27  
28 12 monolithic CEC capillary with 130,000 (N/m) of thioruea. Moreover, a promising resolution,  
29  
30 13 3.8, was observed in the Fig. 5(B), even compared to a resolution of 1.2 observed from the  
31  
32 14 CSP based on covalently bonded chitosan for ligand-exchange liquid chromatography [33].  
33  
34 15 We thus see that MAA-CS is a potential component for CSP as long as a proper buffer  
35  
36 16 condition is used. After more than 400 trials in half a year, the MAA-CS capillary could still  
37  
38 17 afford the 3% and 1% RSD values ( $n=5$ ) for the resolution and selectivity respectively.  
39  
40

41  
42  
43 18 The MAA+CS capillary, which was prepared by an alternative approach for the  
44  
45 19 immobilization of nano-CS on the column, did not achieve enantioseparation of the  
46  
47 20 tryptophans under any of our buffer conditions. This outcome might be attributed to the lacks  
48  
49 21 of CS chiral selectors immobilized in the MAA+CS capillary. Before CS molecules  
50  
51 22 nucleophilically attacked the epoxide rings of the polymerized GMA, some rings might have  
52  
53 23 been opened during the preparation of the polymerization solution, the formation of the  
54  
55 24 polymeric phase with the GMA units, and the waiting time necessary for the polymerization.  
56  
57 25 Another potential reason could arise from the epoxide rings exposed on the solid surface of  
58  
59 26 the polymeric phase. These fixed rings might have been fewer or less reactive to the  
60

1  
2  
3  
4 1 well-dispersed nano-CS in the methylene chloride solution (in the MAA+CS capillary) when  
5  
6 2 compared with the free GMA molecules that homogeneously reacted with nano-CS solution  
7  
8 3 prior to polymerization (in the MAA-CS capillary). In any cases, the MAA+CS capillary  
9  
10 4 would not be used in the following separations.  
11  
12

### 13 3.3 Chiral separation of catechin

14  
15 6 The (+)-(2R,3S)-catechin and (–)-(2S,3R)-catechin belong to the flavonoid group and have  
16  
17 7 different bioavailabilities and bioactivities [50,51]. Their separation is often achieved using  
18  
19 8 cyclodextrin chiral selectors with HPLC, CE, and MEKC methods [52]. Using a CEC method  
20  
21 9 with the MAA-CS capillary, the effect of the pH levels of the phosphate buffer (50 mM, 80%  
22  
23 10 (v/v) MeOH) on the chiral separation of these catechins was found that the optimal pH level  
24  
25 11 seemed to be pH 6.6, at which the electrochromatograms showed the best selectivities. The  
26  
27 12 migration times did not decrease when the EOF magnitude was increased by increases in pH  
28  
29 13 levels of the running buffer, as shown in Fig. 4(A). Thus, a chromatographic retention is likely  
30  
31 14 involved in the separation mechanism. The effect of the ionic strength of the phosphate buffer  
32  
33 15 (pH 6.6, 80% (v/v) MeOH) on the chiral separation of the catechins is shown in Fig. 6. Here  
34  
35 16 the migration times for the MeOH solvent peak and the two catechin peaks increased as the  
36  
37 17 buffer concentration increased, which can be simply explained by the decreased EOF, as  
38  
39 18 shown in Fig. 4(B). Obviously, the selectivity between the (+)-catechin and the (–)-catechin  
40  
41 19 was increased with increasing buffer concentration. However, electrodispersion due to  
42  
43 20 mismatched sample and buffer conductivities resulted in the peak tailing and fronting. After  
44  
45 21 one and half year trial, the resolution,  $R_s = 3.6 (\pm 0.2 (n=5))$ , and selectivity,  $\alpha = 2.5 (\pm 0.1 (n =$   
46  
47 22  $5))$ , were observed in the conditions of Fig. 6(C) with better peak shape.  
48  
49

50  
51  
52  
53  
54 23 The effect of different volume ratios of MeOH in the phosphate buffer (pH 6.6, 50 mM)  
55  
56 24 on the separation of the (±)-catechin in the MAA-CS capillary showed the shortened  
57  
58 25 migration times when increasing the volume percentages of MeOH from 70% to 90% would  
59  
60 26 increase the EOF, as shown in Fig. 4(C). However, the role of the organic modifier not only

1 altered the EOF, but it also affected the chromatographic partitioning between the catechin  
 2 molecules and the MAA-CS phase. Differentiating between the electrophoretic and  
 3 chromatographic contributions to the CEC separation is essential, particularly in this study,  
 4 which focuses on the chiral selectivity induced by nano-CS. Adopting the definition  
 5 formulated by Rathore and Horváth, measures of electrophoretic migration and  
 6 chromatographic retention in CEC can be described by a velocity factor ( $k_e''$ ) and a retention  
 7 factor ( $k''$ ), respectively [53,54]. In brief, they are expressed by equations (1) and (2):

$$k_e'' = \frac{\mu_{ep}}{\mu_{eo2}} \quad (1)$$

$$k'' = \frac{\left[ t_{M2} \times \left( 1 + k_e'' \right) - t_{02} \right]}{t_{02}} \quad (2)$$

10 where  $\mu_{ep}$  and  $\mu_{eo2}$  are the electrophoretic and electroosmotic mobilities. These mobilities can  
 11 be obtained from open-tubular CE experiments on a bare capillary (column 1) and from the  
 12 CEC experiments on the MWNT immobilized capillary (column 2), respectively, as follows:

$$\mu_{ep} = \frac{L_1 \times L_{d1}}{V_1} \times \left( \frac{1}{t_{M1}} - \frac{1}{t_{01}} \right)$$

$$\mu_{eo2} = \frac{L_2 \times L_{d2}}{t_{02} \times V_2}$$

15 where  $L$  is the total column length,  $L_d$  is the distance between the inlet and the detection  
 16 point,  $V$  is the applied voltage,  $t_M$  is the migration time of solute, and  $t_0$  is the migration time  
 17 of DMSO. The plots of velocity and retention factors versus the MeOH modifier percentage  
 18 are shown in Fig. 7.

19 In Fig. 7, the  $k_e''$  values increase with the increase in the MeOH percentage within the  
 20 BGE from 70% to 100%. The electrophoretic properties of analytes should be taken into  
 21 account when their  $pK_a$  values can increase and thus result in higher effective charges ( $q_{eff}$ ).



1  
2  
3  
4 1 Further, the BGE viscosity ( $\eta$ ) values would decrease as more organic modifier was blended  
5  
6 2 with the aqueous medium [55,56]. Based on the equation  $\mu_{ep} = q_{eff}/6\pi\eta r$  where  $r$  is the radius  
7  
8 3 of the analyte ion, the electrophoretic migration of the catechin analytes toward the cathode  
9  
10 4 will be increased while  $q_{eff}$  is increased and  $\eta$  is decreased. This enhanced electrophoretic  
11  
12 5 migration is seen in the upward curve of the  $k_e''$  values shown in Fig. 7, however, the  
13  
14 6 discrimination between the  $k_e''$  values is not sufficient to separate the isomeric pair at any  
15  
16 7 MeOH percentage. On the contrary, there is discrimination between the  $k''$  values in the cases  
17  
18 8 of clear chiral selectivity with 80% and 90% MeOH levels. Moreover, the  $k''$  values increased  
19  
20 9 with increases in the MeOH percentage. Thus, chromatographic retention was observed with a  
21  
22 10 normal-phase mode, which is in agreement with similar results found via HPLC with  
23  
24 11 polysaccharide CSPs [57].

### 12 3.4 Chiral separation of $\alpha$ -tocopherol

13 While  $\alpha$ -tocopherol, a vitamin E class, has 3 chiral centers at the 2, 4' and 8' positions, the  
14 naturally occurring 2R,4'R,8'R- $\alpha$ -tocopherol (RRR- $\alpha$ -tocopherol) is characterized by the very  
15 powerful, biologically active antioxidants. The stereoisomers were determined by off-line  
16 HPLC and GC after their derivatization by acetylation or methylation [58,59]. To examine the  
17 ultimate chiral selective abilities of our developed MAA-CS phase, a racemic  
18 all-rac- $\alpha$ -tocopherol solution without derivatization was used as a test sample. However, only  
19 two peaks were found in the electrochromatograms, as shown in Fig. 8. The pH level and the  
20 addition of the ACN modifier in the borate buffers greatly helped in separating the two peaks.  
21 This situation is analogous to using a chiral polyacrylate and a Chiralpak OT as HPLC  
22 stationary phases to separate  $\alpha$ -tocopherol racemate into two peaks, which correspond to 2R  
23 and 2S stereoisomers [60-62]. In our case, RRR- $\alpha$ -tocopherol was validated as a member of  
24 the latter group corresponding to the second peak. For a better resolution of other group  
25 members, several potential means of improvement are possible including the derivatization of  
26 the samples and the nano-CS.



#### 4 Concluding remarks

Comparison of SEM and ATR-IR spectra taken during the fabrication of an OT-CEC capillary from the graftation of acid-treated nano-CS onto polyacrylamide proved that this new chiral stationary phase was successfully bonded to the capillary wall. The completed MAA-CS capillary was characterized by the measurement of EOF profiles under different running buffer pHs, ionic strengths, and ratios of added organic modifier prior to the separation of chiral samples. For tryptophan, the MAA-CS capillary had satisfactory resolution, which was in contrast with the MAA+CS capillary that had poor resolution. This poor resolution might be caused by the poor loading of CS chiral selectors in the capillary during fabrication. An improved chiral selectivity between ( $\pm$ )-catechins was achieved in a non-aqueous mode by addition of 80% MeOH into the phosphate buffer. As only two peaks were found during the separation of  $\alpha$ -tocopherol stereoisomers, we have recognized that the composition and construction of the MAA-CS capillary may need to be further modified in the future.

*Support of this work by the National Science Council of Taiwan is gratefully acknowledged (NSC-98-2113-M-039-003-MY3).*

#### 5 References

- [1] Gübitz, G., Schmid, M. G., *Electrophoresis* 2007, 28, 114–126.
- [2] Preinerstorfer, B., Lämmerhofer, M., Lindner, W., *Electrophoresis* 2007, 28, 2527–2565.
- [3] Gübitz, G., Schmid, M. G., *J. Chromatogr. A* 2008, 1204, 140–156.
- [4] Preinerstorfer, B., Lämmerhofer, M., Lindner, W., *Electrophoresis* 2009, 30, 100–132.
- [5] Kamande, M. W., Zhu, X. F., Kapnissi-Christodoulou, C., Warner, I. M., *Anal. Chem.* 2004, 76, 6681–6692.
- [6] Kapnissi-Christodoulou, C. P., Lowry, M., Agbaria, R. A., Geng, L., Warner, I. M., *Electrophoresis* 2005, 26, 783–789.
- [7] Kitagawa, F., Kamiya, M., Otsuka, K., *J. Chromatogr. B* 2008, 875, 323–328.

- 1  
2  
3  
4 1 [8] Geng, L., Bo, T., Liu, H., Li, N., Liu, F., Li, K., Gu, J., Fu, R., *Chromatographia* 2004, 59,  
5  
6 2 65–70.  
7  
8  
9 3 [9] Kitagawa, F., Kamiya, M., Okamoto, Y., Taji, H., Onoue, S., Tsuda, Y., Otsuka, K., *Anal.*  
10  
11 4 *Bioanal. Chem.* 2006, 386, 594–601.  
12  
13 5 [10] Han, N.-Y., Hautala, J. T., Bo, T., Wiedmer, S. K., Riekkola, M.-L., *Electrophoresis*  
14  
15 6 2006, 27, 1502–1509.  
16  
17  
18 7 [11] Wiedmer, S. K., Bo, T., Riekkola, M. L., *Anal. Biochem.* 2008, 373, 26–33.  
19  
20 8 [12] Dai, R., Tang, L., Li, H., Deng, Y., Fu, R., Parveen, Z., *J. Appl. Polym. Sci.* 2007, 106,  
21  
22 9 2041–2046.  
23  
24  
25 10 [13] Hu, K., Tian, Y., Yang, H., Zhang, J., Xie, J., Ye, B., Wu, Y., Zhang, S., *J. Liq.*  
26  
27 11 *Chromatogr. Relat. Technol.* 2009, 32, 2627–2641.  
28  
29  
30 12 [14] Shou, C.-Q., Kang, J.-F., Song, N.-J., *Chin. J. Anal. Chem.* 2008, 36, 297–300.  
31  
32 13 [15] Hongjun, E., Yang, Y., Su, P., Zhang, W., *J. Anal. Chem.* 2009, 64, 393–397.  
33  
34 14 [16] Zaidi, S. A., Han, K. M., Kim, S. S., Hwang, D. G., Cheong, W. J., *J. Sep. Sci.* 2009, 32  
35  
36 15 996–1001.  
37  
38  
39 16 [17] Zaidi, S. A., Cheong, W. J., *Electrophoresis* 2009, 30, 1603–1607.  
40  
41 17 [18] Zaidi, S. A., Cheong, W. J., *J. Chromatogr. A* 2009, 1216, 2947–2952.  
42  
43 18 [19] Kitagawa, F., Inoue, K., Hasegawa, T., Kamiya, M., Okamoto, Y., Kawase, M., Otsuka,  
44  
45 19 K., *J. Chromatogr. A* 2006, 1130, 219–226.  
46  
47  
48 20 [20] Olsson, J., Blomberg, J. G., *J. Chromatogr. B* 2008, 875, 329–332.  
49  
50 21 [21] Nilsson, C., Birnbaum, S., Nilsson, S., *J. Chromatogr. A* 2007, 1168, 212–224.  
51  
52 22 [22] Dong, X. L., Wu, R. A., Wu, M. H., Dong, J., Wu, M., Zhuz, Y., Zou, H.,  
53  
54 23 *Electrophoresis* 2008, 29, 3933–3940.  
55  
56  
57 24 [23] Hsieh, Y. L., Chen, T. H., Liu, C. P., Liu, C. Y., *Electrophoresis* 2005, 26, 4089–4097.  
58  
59 25 [24] Li, T., Xu, Y., Feng, Y.-Q., *J. Liq. Chromatogr. Relat. Technol.* 2009, 32, 2484–2498.  
60  
26 [25] Li, H.-F., Zeng, H., Chen, Z., Lin, J.-M., *Electrophoresis* 2009, 30, 1022–1029.

- 1  
2  
3  
4 1 [26] L., Sombra, Moliner-Martínez, Y., Cárdenas, S., Valcárcel, M., *Electrophoresis* 2008, 29,  
5  
6 2 3850–3857.  
7  
8  
9 3 [27] Chen, J.-L., *J. Chromatogr. A* 2010, 1217, 715–721.  
10  
11 4 [28] Kreuter, J., *Nanoparticles. Colloidal Drug Delivery Systems*, Marcel Dekker, New York  
12  
13 5 1994.  
14  
15 6 [29] Lee, K. Y., Kwon, I. C., Kim, Y.-H., Jo, W. H., Jeong, S. Y., *J. Control. Release* 1998,  
16  
17 7 51, 213–220.  
18  
19  
20 8 [30] Huang, X., Wang, Q., Huang, B., *Talanta* 2006, 69, 463–468.  
21  
22 9 [31] Fu, X., Liu, Y., Li, W., Pang, N., Nie, H., Liu, H., Cai, Z., *Electrophoresis* 2009, 30,  
23  
24 10 1783–1789.  
25  
26  
27 11 [32] Kato, M., Saruwatari, H., Sakai-Kato, K., Toyo'oka, T., *J. Chromatogr. A* 2004, 1044,  
28  
29 12 267–270.  
30  
31  
32 13 [33] Liu, Y., Zou, H., Haginaka, J., *J. Sep. Sci.* 2006, 29, 1440–1446.  
33  
34 14 [34] Son, S.-H., Jegal, J., *J. Appl. Polym. Sci.* 2007, 106, 2989–2996.  
35  
36 15 [35] Yamoto, C., Fujisawa, M., Kamigaito, M., Okamoto, Y., *Chirality* 2008, 20, 288–294.  
37  
38 16 [36] Baek, S.-H., Kim, B., Suh, K.-D., *Colloids Surf. A Physicochem. Eng. Asp.* 2008, 316,  
39  
40 17 292–296.  
41  
42  
43 18 [37] Kim, Y. H., Gihm, S. H., Park, C. R., *Bioconjugate Chem.* 2001, 12, 932–938.  
44  
45 19 [38] Chen, J.-L., Lin, Y.-C., *J. Chromatogr. A* 2010, 1217, 4328–4336.  
46  
47  
48 20 [39] He, C., Hendrickx, A., Mangelings, D., Smeyers-Verbeke, J., Heyden, Y. V.,  
49  
50 21 *Electrophoresis* 2009, 30, 3796–3803.  
51  
52 22 [40] Fanalia, S., D'Orazio, G., Lomsadzeb, K., Samakashvilib, S., Chankvetadze, B., *J.*  
53  
54 23 *Chromatogr. A* 2010, 1217, 1166–1174.  
55  
56  
57 24 [41] Smoluchowski, Mv., *Handbuch der Elektrizität und des Magnetismus*, Barth, Liepzig  
58  
59 25 1921.  
60  
26 [42] Rice, C., Whitehead, R., *J. Phys. Chem.* 1965, 69, 4017–4024.

- 1  
2  
3  
4 1 [43] Hiemenz, P. C., Rajagopalan, R., *Principles of Colloid and Surface Chemistry*, Marcel  
5  
6 2 Dekker, New York 1997.  
7  
8 3 [44] Lyklema, J., Minor, M., *Colloids Surf. A Physicochem. Eng. Asp.* 1998, *140*, 33–41.  
9  
10 4 [45] Rathore, A. S., Wen, E., Horváth, Cs., *Anal. Chem.* 1999, *71*, 2633–2641.  
11  
12 5 [46] Huang, X., Zhang, J., Horváth, Cs., *J. Chromatogr. A* 1999, *858*, 91–101.  
13  
14 6 [47] Chen, J.-L., *Electrophoresis* 2006, *27*, 729–735.  
15  
16 7 [48] Chen, J.-L., *Electrophoresis* 2009, *30*, 3855–3862.  
17  
18 8 [49] Chen, J.-L., *J. Chromatogr. A* 2009, *1216*, 6236–6244.  
19  
20 9 [50] Donovan, J. L., Crespy, V., Oliveira, M., Copper, K. A., Gibson, B. B., Williamson, G.,  
21  
22 10 *Free Radic. Res.* 2006, *40*, 1029–1034.  
23  
24 11 [51] Nyfeler, F., Moser, U. K., Walter, P., *Biochim. Biophys. Acta* 1983, *763*, 50–57.  
25  
26 12 [52] Kim, H., Choi, Y., Lim, J., Paik, S.-R., Jung, S., *Chirality* 2009, *21*, 937–942.  
27  
28 13 [53] Rathore, A. S., Horváth, Cs., *J. Chromatogr. A* 1996, *743*, 231–246.  
29  
30 14 [54] Rathore, A. S., Horváth, Cs., *Electrophoresis* 2002, *23*, 1211–1216.  
31  
32 15 [55] Porras, S. P., Kenndler, E., *J. Chromatogr. A* 2004, *1037*, 455–465.  
33  
34 16 [56] Wright, P. B., Lister, A. S., Dorsey, J. G., *Anal. Chem.* 1997, *69*, 3251–3259.  
35  
36 17 [57] Bielejewska, A., Duszczuk, K., Kulig, K., Malawska, B., Miśkiewicz, M., Leś, A.,  
37  
38 18 Zukowski, J., *J. Chromatogr. A* 2007, *1173*, 52–57.  
39  
40 19 [58] Usda, T., Ichikawa, H., Igarashi, O., *J. Nutr. Sci. Vitaminol.* 1993, *39*, 207–219.  
41  
42 20 [59] Klaczko, G., Anuszevska, E., *Acta. Pol. Pharm.* 2008, *65*, 715–721.  
43  
44 21 [60] Vecchi, M., Walther, W., Glinz, E., Netscher, T., Schmid, R., Lalonde, M., Vetter, W.,  
45  
46 22 *Helv. Chim. Acta* 1990, *73*, 782–789.  
47  
48 23 [61] Yamaguchi, H., Itakura, Y., Kunihiro, K., *Iyakuhi Kenkyu* 1984, *15*, 536–540.  
49  
50 24 [62] Ueda, T., Ichikawa, H., Igarashi, O., *J. Nutr. Sci. Vitaminol.* 1993, *39*, 207–219.  
51  
52  
53  
54  
55  
56  
57  
58  
59  
60

## 1 Figure captions and legends

2 **Figure 1.** Chemical structures of the chiral samples.

3 **Figure 2.** Schemes to synthesize the CS-immobilized capillary.

4 **Figure 3.** SEM images. (A) Acid-treated nano-CS; (B) nano-CS/polyacrylamide composite  
5 (MAA-CS powder); (C) coatings around a cut rim of the MAA-CS capillary; and (D) coatings  
6 on the inner wall of the MAA-CS capillary.

7 **Figure 4.** Dependence of electroosmotic mobility on buffer pH, ionic strength, and the ratio  
8 of organic modifier. Columns: (□) a bare fused-silica capillary; (○) and (●) the MAA-CS  
9 capillary. BGE conditions: phosphate buffer, (A) 50 mM; (B) pH 7.5; (C) 10 mM, pH 7.5.

10 Sample: DMSO; hydrostatic injection of 10 cm for 1 sec and detection at 214 nm. The applied  
11 voltage was 10 kV. The symbols (○) and (●) in (C) represent the BGE mixing with ACN and  
12 MeOH, respectively, and their corresponding  $\epsilon/\eta$  values are denoted by (◇) and (◆).

13 **Figure 5.** Enantioseparations of the tryptophans in the MAA-CS capillary of (60 cm (55 cm)  
14 x 75  $\mu\text{m}$  I.D.). Conditions: BGE, Tris buffer, 100 mM at pH equals (A) 8.5, (B) 9.5, (C) 10.5,  
15 and (D) 9.5 with the addition of 10% (v/v) MeOH. The applied voltage was 15 kV. Samples:  
16 hydrostatic injection of 10 cm for 5 sec and detection at 214 nm. Peak correspond to (1)  
17 D-tryptophan and (2) L-tryptophan.

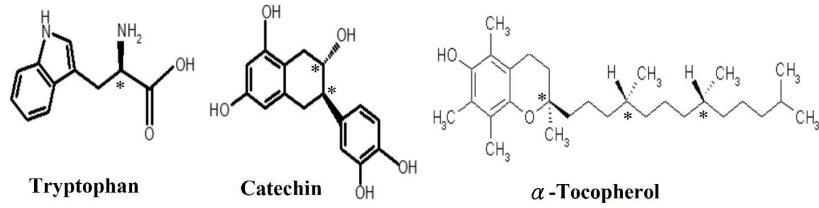
18 **Figure 6.** Chiral separations of catechins with different buffer concentrations in the MAA-CS  
19 capillary (45 cm (42 cm) x 75  $\mu\text{m}$  I.D.). Conditions: BGE, MeOH (80%, v/v) and phosphate  
20 buffer, pH 6.6, at buffer concentration equals (A) 10 mM, (B) 50 mM, (C) 70 mM, and (D) 90  
21 mM. The applied voltage was 15 kV. Samples: hydrostatic injection of 10 cm for 5 sec and  
22 detection at 280 nm. Peak correspond to (S) MeOH, (1) (-)-catechin, and (2)

23 (+)-catechin. **Figure 7.** Effect of the addition of MeOH into the phosphate buffer (pH 6.3, 100  
24 mM) on the velocity factor ( $k_e''$ ) and the retention factor ( $k''$ ) of ( $\pm$ )-catechins. CEC  
25 conditions are the same as in Fig. 6(B). (○) and (□) represent the  $k_e''$  values of (-)-catechin  
26 and (+)-catechin, respectively. (●) and (■) represent the  $k''$  values of (-)-catechin and

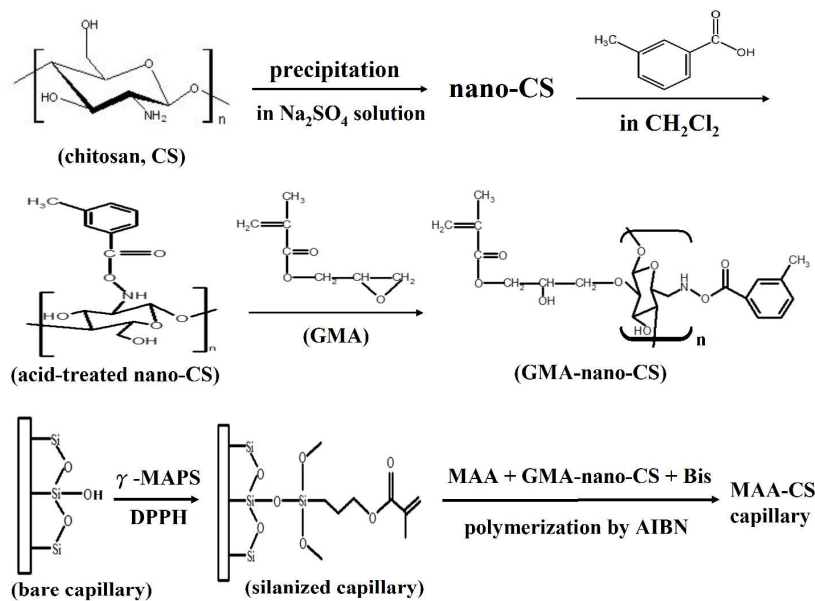
1 (+)-catechin, respectively.

2 **Figure 8.** Chiral separations of racemic  $\alpha$ -tocopherols in the MAA-CS capillary (52 cm (47  
3 cm) x 75  $\mu$ m I.D.). Conditions: BGE, borate buffer, 100 mM, at pH equals (A) 7.5, (B) 8.5,  
4 (C) 9.5, and (D) pH 8.5 with addition of 10% (v/v) ACN. The applied voltage was 10 kV.  
5 Samples: hydrostatic injection of 10 cm for 5 sec and detection at 200 nm. Peak assignments:  
6 (1) Group 1, (2) Group 2 containing (+)-2*R*,4'*R*,8'*R*- $\alpha$ -tocopherol.

For Peer Review

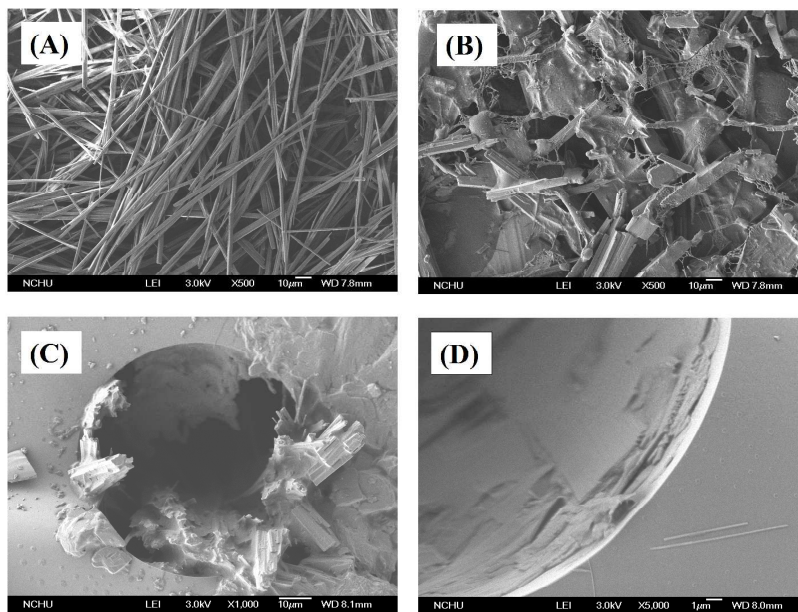


297x209mm (300 x 300 DPI)

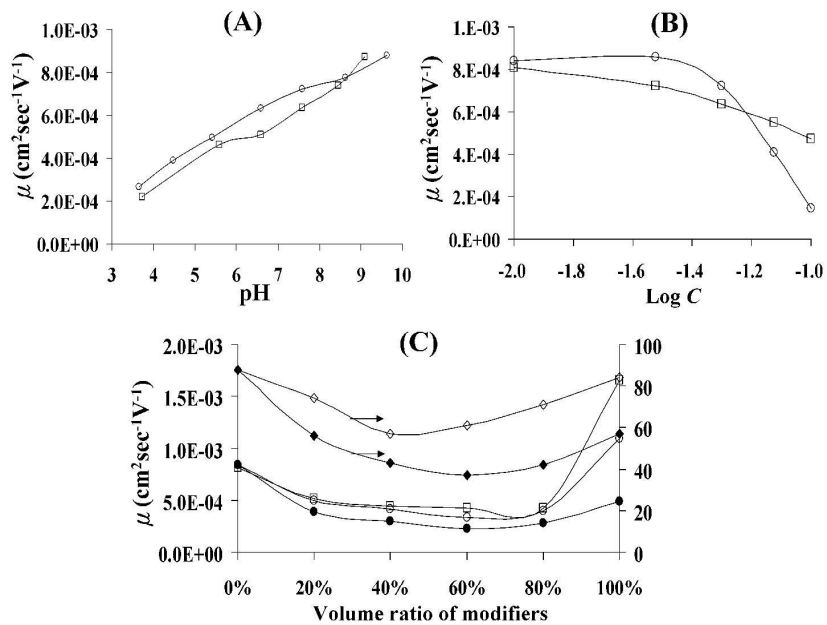


297x209mm (300 x 300 DPI)

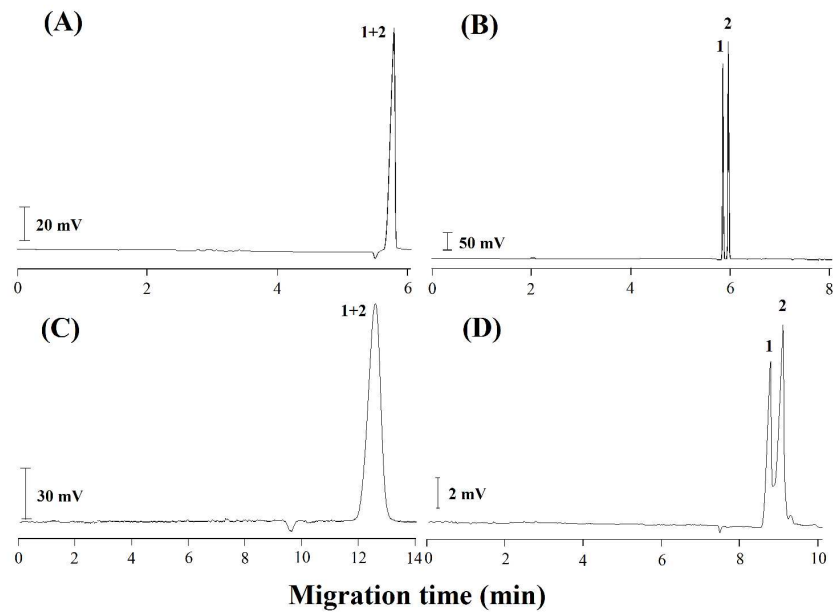




297x209mm (300 x 300 DPI)

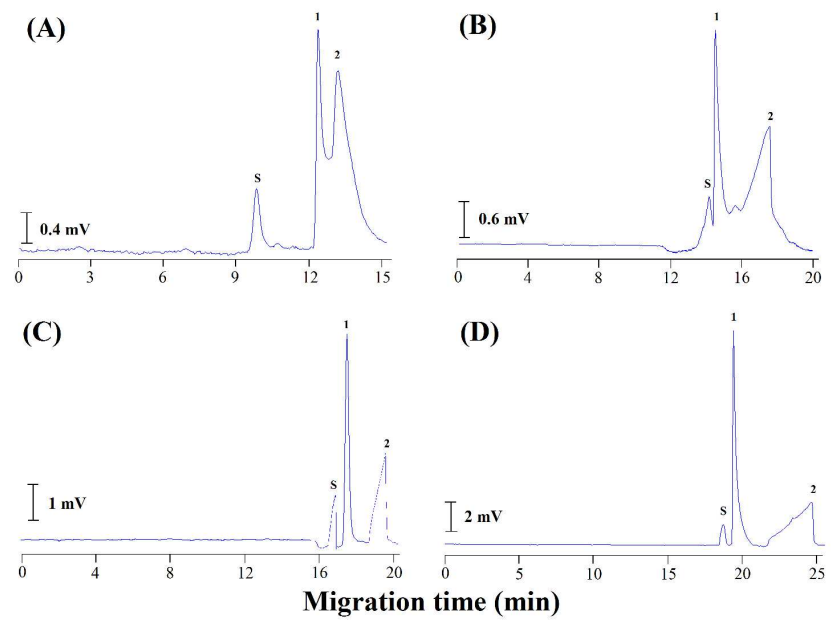


297x209mm (300 x 300 DPI)



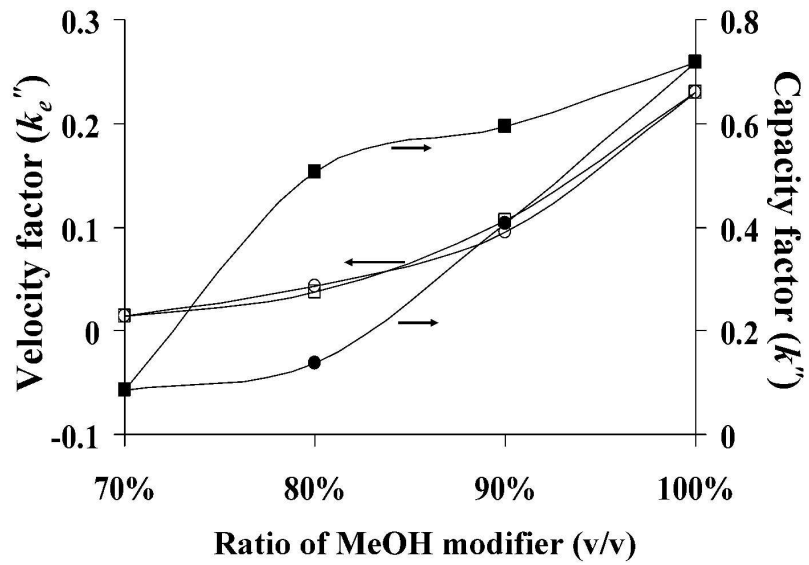
297x209mm (300 x 300 DPI)

1  
2  
3  
4  
5  
6  
7  
8  
9  
10  
11  
12  
13  
14  
15  
16  
17  
18  
19  
20  
21  
22  
23  
24  
25  
26  
27  
28  
29  
30  
31  
32  
33  
34  
35  
36  
37  
38  
39  
40  
41  
42  
43  
44  
45  
46  
47  
48  
49  
50  
51  
52  
53  
54  
55  
56  
57  
58  
59  
60

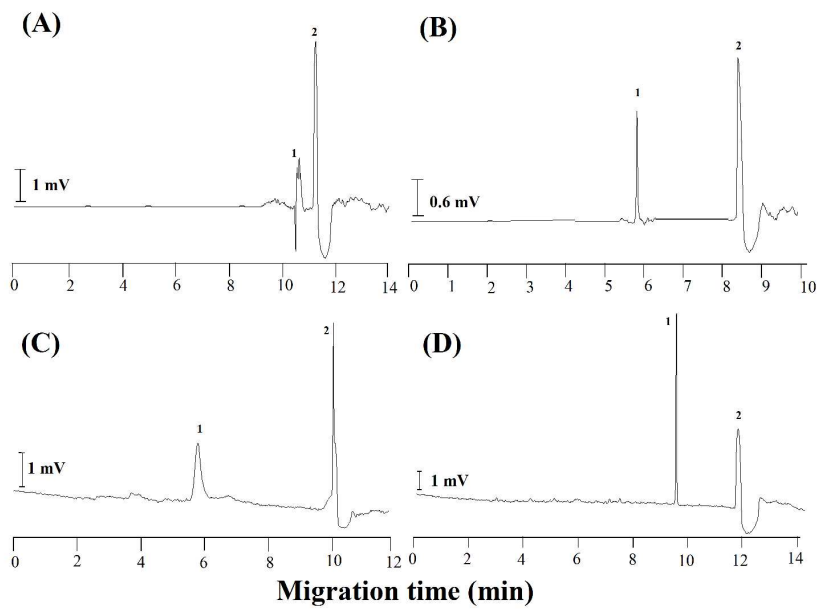


297x209mm (300 x 300 DPI)

review



297x209mm (300 x 300 DPI)



297x209mm (300 x 300 DPI)